

Synthesis and Biophysical Studies of High-Affinity Morpholino Oligomers Containing G-Clamp Analogs

Arnab Das, Atanu Ghosh, Jayanta Kundu, Martin Egli, Muthiah Manoharan, and Surajit Sinha*



Cite This: *J. Org. Chem.* 2023, 88, 15168–15175



Read Online

ACCESS |



Metrics & More

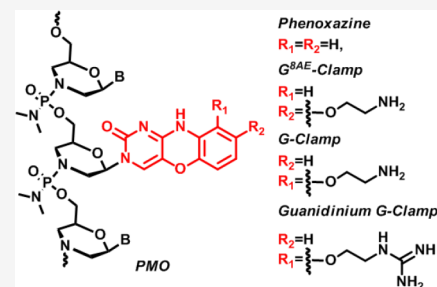


Article Recommendations



Supporting Information

ABSTRACT: Successful syntheses of chlorophosphoramidate morpholino monomers containing tricyclic cytosine analogs phenoxazine, G-clamp, and G^{8AE}-clamp were accomplished. These modified monomers were incorporated into 12-mer oligonucleotides using trityl-chemistry by an automated synthesizer. The resulting phosphorodiamidate morpholino oligomers, containing a single G-clamp, demonstrated notably higher affinity for complementary RNA and DNA compared to the unmodified oligomers under neutral and acidic conditions. The duplexes of RNA and DNA with G-clamp-modified oligomers adopt a B-type helical conformation, as evidenced by CD-spectra and show excellent base recognition properties. Binding affinities were sequence and position dependent.



INTRODUCTION

To make nucleic acids suitable for therapeutic purposes, they must be chemically modified to increase affinity for complementary RNA strands and to improve nuclease resistance and cellular uptake.^{1–5} The fundamental basis of biomolecular recognition lies in Watson–Crick base pairing during duplex formation. Increased affinity can be achieved by improving stacking interactions and/or hydrogen bonding.^{6–10} Enhanced stacking can be accomplished by introducing polycyclic nucleobase analogs, and the number of H-bonds can be increased by engineering the simultaneous recognition of both the Watson–Crick and Hoogsteen binding faces of guanine and adenine bases. In a cytosine–guanine pair, the guanine has two unused H-bond acceptors in the major groove at the O6 and N7 atoms.^{11,12} To form H-bonds with these acceptors, a tricyclic cytosine analog with an aminoethoxy-derivatized phenoxazine ring was designed by Matteucci (Figure 1).^{11,12} This cytosine analog, referred to as the amino-G-clamp (G-clamp), was incorporated into oligonucleotides and shown to enhance duplex stability.^{11–16} The proposed four H-bonds are shown in Figure S1. The amino group of the G-clamp has been converted to the guanidinium group which exhibits unique pairing via five H-bonds with the opposite G by utilizing the O6 and N7 atoms, as confirmed by X-ray crystallography (Figure S1).^{17,18}

In the case of PNA, G-clamp modifications result in the highest affinity for complementary DNA and RNA targets reported so far for PNA modifications.¹⁹ G-clamps have also been used to modify 2'-O-methyl-modified RNA²⁰ and LNA.²¹

Phosphorodiamidate morpholino oligomers (PMOs) are nucleic acid analogs based on morpholine rings joined by neutral phosphorodiamidate linkages. Developed by Summer-ton, PMOs have clinically proven therapeutic activity as splicing modulators.²² In 2016, Eteplirsen became the first

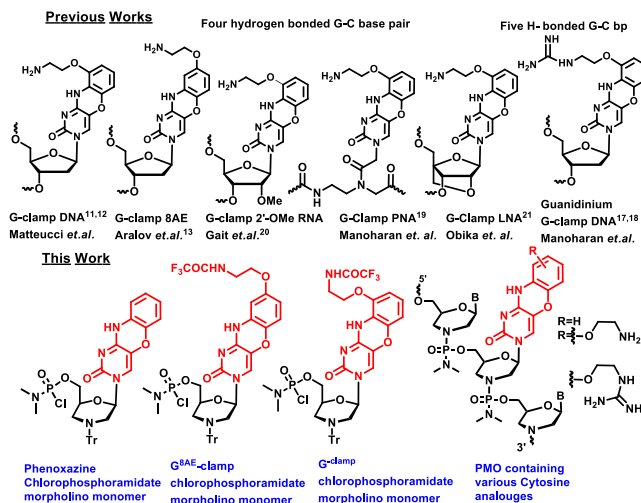


Figure 1. Previously reported G-clamps and chlorophosphoramidate morpholino monomers synthesized for this work.

PMO-based FDA-approved drug for clinical use. It modulates splicing to treat Duchenne muscular dystrophy (DMD). Three additional PMO drugs are approved for the treatment of subtypes of DMD.^{22b,c} Since longer sequences of PMO are used for therapeutic applications compared to those based on RNA, further modification may be required. For example, the

Received: July 25, 2023

Published: October 16, 2023



antisense oligonucleotide Nusinersen is an 18-mer, whereas Eteplirsen is a 30-mer. Thus, modifications that enhance the binding affinity of the PMO are highly desirable. To improve the binding affinity of the PMOs, we prepared suitably protected amino- and guanidino-G-clamps, G^{8AE}-clamp, and phenoxazine morpholino (MO) monomers (Figure 1) and evaluated hybridization properties and other characteristics of PMOs containing these modifications. The inclusion of such modified monomers in a shorter oligomer has the potential to replicate the binding efficiency of a longer oligomer.

RESULTS AND DISCUSSION

Compound **1a** was synthesized according to the previously reported method.²³ NBS/pyridine-mediated bromination of **1a**

Scheme 1. Synthesis of the Morpholino 5-Bromouridine

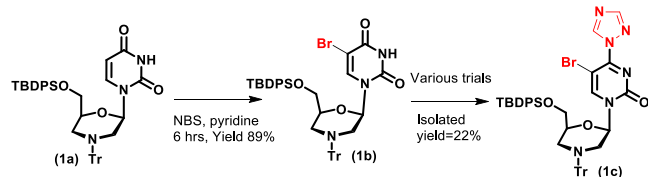
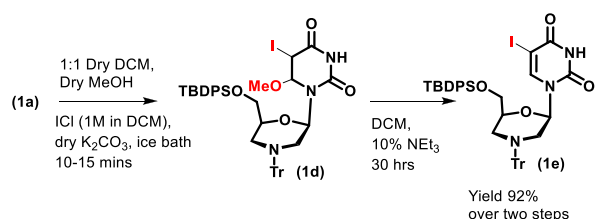


Table 1. C4 Activation of **1b** under Various Conditions

entry ^a	reaction condition	result at 24 h	
activator	additive		
1	POCl ₃ (3 equiv)	1,2,4-triazole (10 equiv)	no reaction
2	POCl ₃ (5 equiv)	1,2,4-triazole (17 equiv)	no reaction
3 ^b	PPh ₃ (1.5 equiv)		no reaction
4	POCl ₃ (5 equiv)	NMI (32 equiv)	60% conversion to 1c
5	POCl ₃ (10 equiv)	NMI (32 equiv)	25% conversion to 1c ; 55% 1b

^aSolvent, CH₃CN; base, Et₃N. ^bDCM–CCl₄ (1:1) under reflux (oil bath), DIPEA (2.5 equiv). NMI–1-methylimidazole.

Scheme 2. Synthesis of the Morpholino 5-Iodoouridine



yielded compound **1b** in high yield (89%) (Scheme 1). We next attempted to incorporate the substituted aminohydroquinone at C4 of the uracil moiety. However, the direct incorporation of substituted aminophenol by the activation of C4 with PPh₃-CCl₄ followed by a reaction with the aromatic amine in the presence of DBU failed. POCl₃/1,2,4-triazole mediated activation also did not give the desired compound **1c** in a promising yield. POCl₃/Et₃N-mediated activation shows the decomposition of the material. Finally, POCl₃/1-methylimidazole (NMI) mediated activation of C4, followed by the addition of 1,2,4-triazole showed complete consumption of the starting material. However, the compound was found to revert to the starting material during column chromatographic purification, yielding **1c** in poor yield.

Scheme 3. Synthesis of the Morpholino G^{8AE}-Clamp

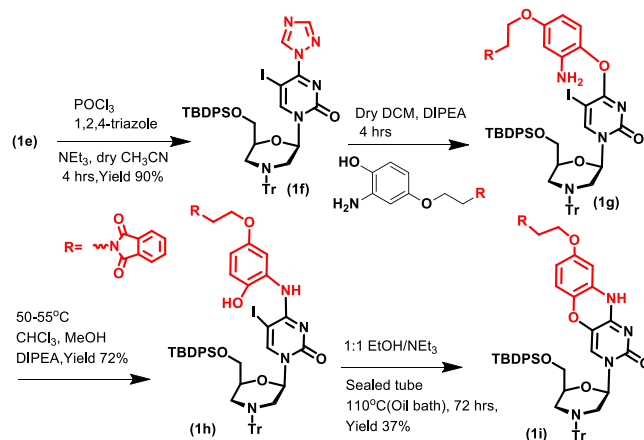
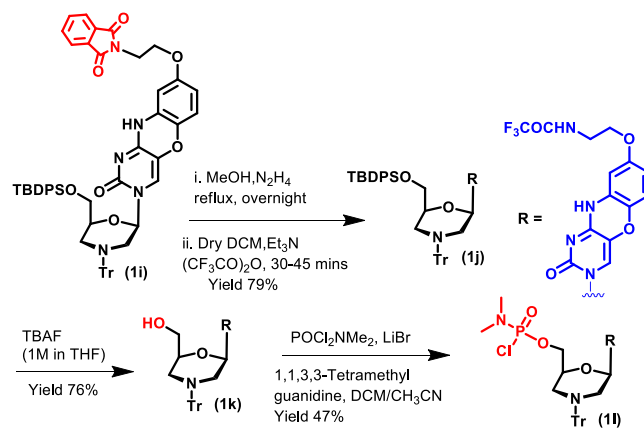


Table 2. Optimization of the Cyclization Reaction

entry	reaction conditions	result
1	absolute EtOH, DBU (or TMG), room temperature	no reaction
2	methanolic NH ₃	no reaction
3	DIPEA, EtOH	
4	MeOH, NH ₄ OH	
5	K ₂ CO ₃ (or Cs ₂ CO ₃), DMF, 100 °C	decomposition of 1h
6	EtOH, AgCN, reflux	no reaction
7	CsF, Cs ₂ CO ₃ , EtOH, reflux	
8	n-BuOH, EtOH, reflux	
9	EtOH, Et ₃ N, reflux	trace 1i
10	MeOH or EtOH, Et ₃ N, sealed tube, 110 °C	desired compound 1i

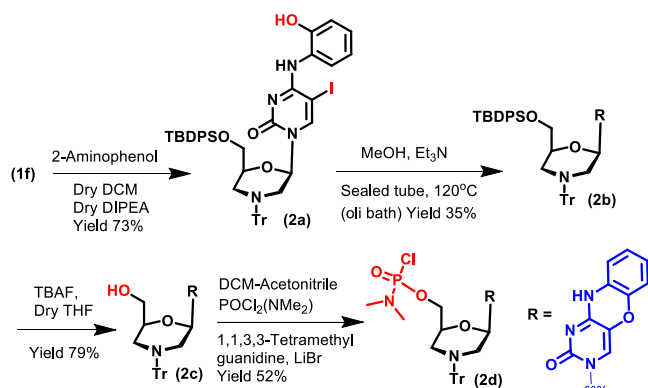
Scheme 4. Synthesis of the Morpholino G^{8AE}-Clamp Chlorophosphoramidate Monomer



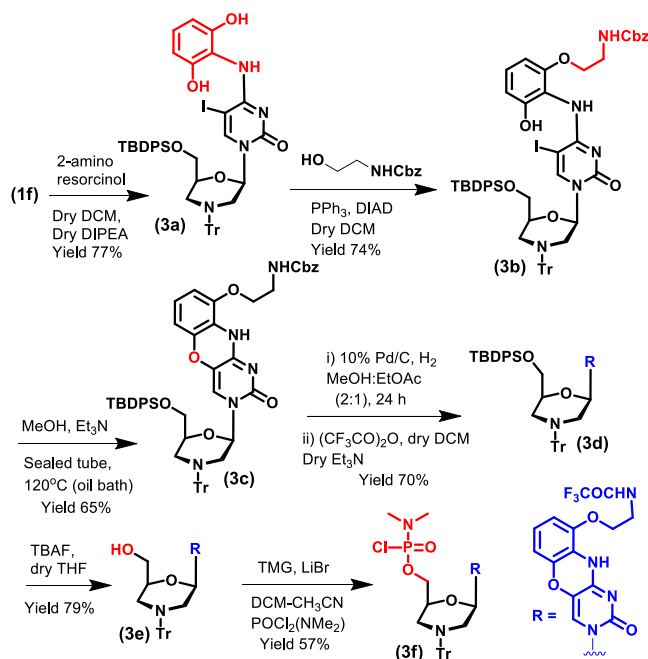
Since the conversion of **1c** from the bromo derivative **1b** was found to be poor (Table 1), we modified our approach by using the iodo derivative and synthesized **1e** (Scheme 2).

The C4 triazole **1f** was synthesized using POCl₃/1,2,4-triazole in 90% yield (Scheme 3) which reflects the robustness of the iodo derivative over the bromo in the case of morpholino monomers. Treatment of **1f** with substituted aminohydroquinone (Scheme S1) gave **1g** as the major product. **1g** slowly isomerizes through a Smiles rearrangement to thermodynamically more stable **1h**, demonstrated by NMR

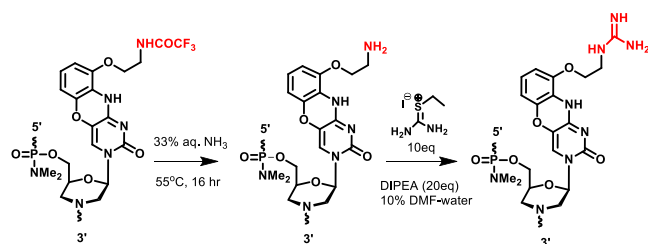
Scheme 5. Synthesis of the Morpholino Tricyclic Phenoxazine Chlorophosphoramidate Monomer



Scheme 6. Synthesis of the Morpholino G-Clamp Chlorophosphoramidate Monomer



Scheme 7. Synthesis of the Guanidinium G-Clamp PMO



spectroscopy (SI). The next challenge was the intramolecular cyclization of **1h**.

After screening various conditions (Table 2), we found that heating **1h** in a sealed tube at 110 °C (oil bath) for 72h gave the desired **1i** in 37% yield. Phthalimide deprotection by hydrazine hydrate followed by the protection of the free amine using trifluoroacetic anhydride (TFAA) gave **1j** (Scheme 4).

Tetrabutylammonium fluoride (TBAF)-mediated deprotection of the TBDPS group yielded **1k** (Scheme 4). The

chlororophosphoramidate monomer **1l** was synthesized using the LiBr-TMG method reported previously.²⁴ Phenoxazine derivatives (**2b–d**) were synthesized using a similar strategy (Scheme 5).

To synthesize the morpholino G-clamp chlorophosphoramidate monomer **3f** (Scheme 6), **1f** was treated with 2-aminoresorcinol, yielding **3a**. *N*-phthalimide-protected ethanolamine was subjected to various Mitsunobu conditions, but the reaction failed. NH-Cbz-protected ethanolamine in the presence of DIAD/PPh₃ in THF gave the monosubstituted product **3b** along with a very minute amount of diprotected product.

3b was then cyclized to give **3c** as mentioned earlier for **2b**. Cbz was deprotected by 10% Pd/C under a H₂ atmosphere. The free amine was purified and protected with trifluoroacetamide to obtain **3d**. After TBDPS deprotection, **3e** was converted to **3f** as discussed earlier.

The chlorophosphoramidate monomers were used in the synthesis of two 12-mer PMOs (5'-TTTTACTCACAT-3' and 5'-TGTCATCCATT-3', the bold letters are the sites of a single modification) on Ramage Chemmatrix resin following the reported procedure (Figure S2).^{24,25} The PMOs were purified by HPLC and characterized by MALDI-TOF (Table S1 and Figures S3–S15). A postsynthetic strategy was adopted for the conversion of amine to guanidinium group as previously reported.²⁶ After the synthesis of PMO, the resin was treated with a 33% aqueous NH₃ solution. The supernatant was lyophilized and treated with 2-ethylthiuronium iodide in the presence of DIPEA in 10%-DMF/water at 55 °C for 24 h (Scheme 7) to obtain guanidinium PMO (PMO-5, **10** and **14**).

Inflection points from the first derivative plot of thermal melting curves (*T_m*s) were determined for the modified and unmodified 12-mer PMOs with complementary DNA and RNA, respectively (Table 3 and Figures S16–S28).

Incorporation of phenoxazine (X) in PMO-2 greatly enhanced the RNA-PMO duplex stability when the *T_m* of the PMO-2 duplex was compared to that of the duplex with unmodified PMO; however, slight destabilization was observed in the case of PMO-7 and PMO-11. The phenoxazine is hydrophobic and may have unfavorable dehydration effects on the groove during duplex formation in certain sequence contexts. *T_m* values for the phenoxazine and its analogs were previously reported to be sequence-dependent.¹⁵ Incorporation of G^{8AE}-clamp Y in PMO-3, PMO-8, and PMO-12 increased the *T_m* values relative to the unmodified PMO by between +15.4, +10.5, and +6.1 °C, respectively. Varizhuk et al.¹³ have reported the ionic strength-dependent binding affinity of the G^{8AE}-clamp, whereas the G-clamp showed its salt-independent behavior. This reflects that the interstrand ionic interaction plays a major role for the former whereas the sole H-bonding interaction was responsible for the latter observation. A model of the Y:G pair shows that the AE amino group of Y (in PMO) can approach the O6 atom of the paired G (ca. 3.5 Å; Figure 2A). Potential H-bond formation between the 8AE amino nitrogen and O6 of the paired G is shown in Figure 2B. In this model, (Figure 2A), it is slightly outside the distance range that would allow effective H-bond formation. However, the introduction of a positively charged moiety into the center of the major groove, a site of strong negative electrostatic surface potential (ESP), and in the vicinity of the O6/N7 edge of G, still affords a stabilizing effect as per the *T_m* data. Moreover, incorporation of the G-clamp and the G^{8AE}-

Table 3. T_m of Modified PMOs with complementary DNA and RNA^a

PMO number	sequence	T_m with complementary DNA (°C)	ΔT_m	T_m with complementary RNA (°C)	ΔT_m
PMO-1 ²⁵	5'-TTTTACTCACAT-3'	26		24	
PMO-2	5'-TTTTACTXACAT-3'	30.2	+4.2	33.9	+9.9
PMO-3	5'-TTTTACTYACAT-3'	34.5	+8.5	39.4	+15.4
PMO-4	5'-TTTTACTZACAT-3'	44.0	+18.0	52.4	+28.4
PMO-5	5'-TTTTACTWCAT-3'	40.6	+14.6	48.4	+24.4
PMO-6	5'-TGTCATCCCATT-3'	41.2		50.3	
PMO-7	5'-TGTXATCCCATT-3'	39.2	-2	46.5	-3.8
PMO-8	5'-TGYATCCCATT-3'	47.6	+6.4	60.8	+10.5
PMO-9	5'-TGTZATCCCATT-3'	54.2	+13.0	66.9	+16.6
PMO-10	5'-TGTWATCCCATT-3'	46.6	+5.4	59.8	+9.5
PMO-11	5'-TGTCATCXCAT-3'	43.7	+2.5	49.2	-1.1
PMO-12	5'-TGTCATCYCAT-3'	48.2	+7.0	56.4	+6.1
PMO-13	5'-TGTCATCZCAT-3'	60.2	+19.0	69.0	+18.7
PMO-14	5'-TGTCATCWCAT-3'	56.6	+15.4	63.8	+13.5

^aX = 2d, phenoxazine, Y = 1l, G^{8AE}-clamp, Z = 3f, G-clamp, W = guanidino G-clamp. Conditions: 40 mM phosphate buffer (pH 7). The concentration of each strand was 1 μ M. The T_m values reported are the averages of two independent experiments, and results differed by less than $\pm 1.0^\circ$. The ΔT_m values are in comparison to those of unmodified PMO-1 or PMO-6.

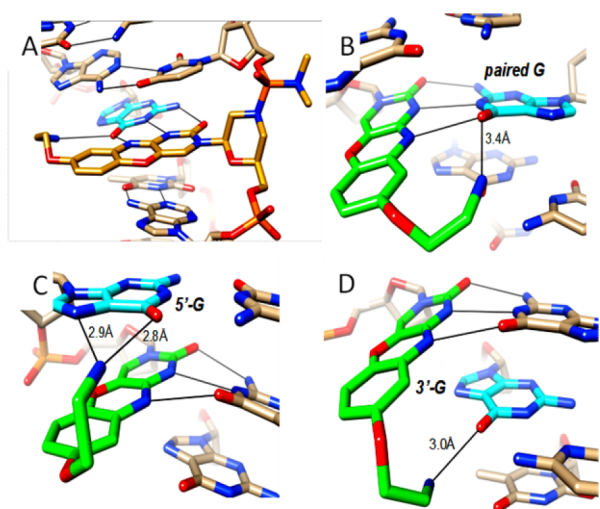


Figure 2. Computational models of G^{8AE}-clamp interactions. (A) of PMO G^{8AE}-clamp Y:G pairing. The AE amino nitrogen is positioned at ca. 3.5 Å from O6 of G. PMO and guanine carbon atoms are highlighted in golden rod and cyan, respectively, and H-bonds are shown as thin solid lines. Three hypothetical interaction modes of the G^{8AE}-clamp are observed in the 5'-G[G^{8AE}-clamp]G-3' sequence context. (B) G^{8AE}-clamp Y:G pairing based on the crystal structure of the guanidino G-clamp modified DNA decamer duplex shown in Figure S1A, with a potential H-bond formation between 8AE amino nitrogen and O6 of the paired G. (C) H-bond interaction between the G^{8AE}-clamp and O6 and N7 of 5'-intrastrand G. (D) H-bond interaction between the G^{8AE}-clamp and O6 of the 3'-intrastrand G. Y carbon atoms are colored in green, and the color code for all other atoms is identical to that in Figure S1. H-bonds between the Y 8AE amino group and the Hoogsteen edge of Gs are shown as thin solid lines with distances in Å.

clamp may produce stability-enhancing effects that differ from those seen for the guanidino G-clamp (H-bonds to O6 and N7 of the paired G, Figure S1A).^{14,15}

Thus, the G- and G^{8AE}-clamp amino group could also scan the major groove edges of bases from 5'- and 3'-adjacent residues (e.g., intrastrand for G^{8AE}, Figure 2C,D). The different positions of substituents in the G- and G^{8AE}-clamps could affect the ability to reach 5'- and 3'-adjacent bases from either the same (intrastrand) or the opposite strand (interstrand).

Compared to the G^{8AE}-clamp, the orientation of the substituent in the G-clamp could aid in reaching the O6 atoms of 5'- and 3'-adjacent guanines from the opposite strand (Figure S1B).

By comparison, the guanidino moiety of the guanidino G-clamp may be lodged exclusively opposite the major groove edge of the paired G (Figure S1A). The promiscuity of the (amino) G-clamp may be an underappreciated feature that distinguishes it from the guanidino G-clamp. The term clamp may be more appropriate for the latter, whereas the original G-clamp could boost the stability in a sequence-dependent manner: H-bonding to the paired G, the major groove edges of bases one step up or down from the opposite strand and inserting a positive charge into a region of negative ESP. This could explain the previous observation whereby the G-clamp typically results in higher T_m gains than the guanidino G-clamp.

This is confirmed here by the thermal melting data for the PMO-modified duplexes. Thus, incorporation of the G-clamp Z increased the T_m by +28.4 °C, +16.6 °C (PMO-4 and PMO-9, respectively). However, the stabilization was reduced by comparison for PMO-5 and PMO-10 (T_m was +24.4 and +9.5 °C, respectively). PMO-13, in which the G-clamp is located between two cytosines, is of higher stability than PMO-9 (RNA: +18.7 vs +16.6 °C, respectively). Similarly, in this case, G-clamp was found to be more stabilizing than the corresponding guanidino version, although the location between two cytosines also led to higher stability for the guanidino G-clamp (RNA: PMO-14 +13.5 °C vs PMO-10 +9.5 °C). This difference between the two clamps also exists in the DNA context.

The sequence-dependent effect is worth noting because the contribution from base-stacking is diminished by the position of the clamps between Cs. Thus, in RNA, phenoxazine-modified (X) PMO-11 displays a lower stability relative to the parent oligo PMO-6 (-1.1 °C), whereas PMO-2 with X is significantly more stable than the parent PMO-1 (+9.9 °C). This gap of 11 °C accounts nicely for the different stabilizations between PMO-3 and PMO-12 (Y), between PMO-4 and PMO-13 (Z), and between PMO-6 and PMO-14 (W).

Table 4. T_m of the PMO-containing Duplexes at Different pH Values^a

PMO number	PMO–DNA duplex				PMO–RNA duplex			
	pH 7	pH 5.5	pH 4	$\Delta\Delta T_m$	pH 7	pH 5.5	pH 4	$\Delta\Delta T_m$
PMO-1	26	27.1	22.4		24	28.8	23.1	
PMO-2	30.2	30.3	25.4	−1.2	33.9	32.4	26.4	−6.6
PMO-3	34.5	34.4	27.8	−3.1	39.4	36.1	28.6	−9.9
PMO-4	44.0	44.7	41.9	1.5	52.4	54.3	49.5	−2
PMO-5	40.6	39.3	37.2	0.2	48.4	49.5	43.2	−4.3
PMO-6	41.2	40.6	33.1		50.3	49.1	40.4	
PMO-11	43.7	43.3	35.9	0.3	49.2	49.8	43.7	4.4
PMO-12	48.2	49.6	41.8	1.7	56.4	57.7	52.0	5.5
PMO-13	60.2	60.4	56.0	3.9	69.0	70.3	65.9	6.8
PMO-14	56.6	58.1	54.8	6.3	63.8	64.2	60.4	6.5

^a $\Delta\Delta T_m = [\Delta T_m(\text{pH } 4) - \Delta T_m(\text{pH } 7)]$. Conditions: 40 mM phosphate buffer (pH 4, 5.5, or 7). The concentration of each strand was 1 μM . The T_m values reported are the averages of two independent experiments and results differed by less than $\pm 1.0^\circ$.

Table 5. T_m of Unmodified PMO and PMO with a G-Clamp with Fully Complementary (G) and Mismatched DNA and RNA^a

sequence	dG	T_m with DNA ($^\circ\text{C}$)		
		dC	dA	dT
PMO-6	41.2			
PMO-11	43.7	23.4	27.7	21.6
PMO-12	48.2	30.1	31.6	30.3
PMO-13	60.2	34.8	29.7	35.8
PMO-14	56.6	33.3	31.0	32.0
sequence	rG	T_m with RNA ($^\circ\text{C}$)		
		rC	rA	rU
PMO-6	50.3			
PMO-11	49.2	25.1	30.4	25.5
PMO-12	56.4	28.6	35.4	32.1
PMO-13	69.0	39.0	37.6	38.3
PMO-14	63.8	32.3	34.3	29.4

^aConditions: Reported in Table 1. Each strand was 1 μM . The T_m values reported are the averages of two independent experiments, and results differed by less than $\pm 1.0^\circ$. Mismatch DNA: 5'-AATGBGATGACA-3'; Mismatch RNA: 5'-AATGBGATGACA-3, where "B" denotes the mismatched base.

As eluded to above, the sequence-dependent, higher stability afforded by G-clamp Z and guanidino G-clamp W wedged between cytosines can be rationalized by potential interstrand H-bonding interactions between amino and guanidino moieties, respectively, and O6 atoms of 5'- and 3'-adjacent guanines in addition to those with the paired G. Figure S1 depicts the guanidino G-clamp (panel A) and G-clamp (panel B) wedged between Gs, the reader can imagine that the respective substituents could reach the O6 atoms of Gs positioned one step up and down on the opposite strand (Cs in the present illustration). As before, the more pronounced effect with regard to stability seen in the case of the G-clamp is likely due to the ability of the positively charged substituent to better scan the major groove edges of Gs from the opposite strand relative to the guanidino G-clamp substituent.

The T_m data also allow a potential conclusion regarding the difference between the sequence-dependence of stability afforded by G-clamp and G^{SAE}-clamp and the relative abilities of their substituents to interact via H-bonds with guanines one step up or down in either the intra- or the interstrand fashion. Thus, the G-clamp substituent is directed more toward the center of the major groove, whereas the substituent of the

G^{SAE}-clamp juts out almost perpendicularly relative to the major groove base edges. Indeed, the stability gain for PMO-12 is significantly lower than that for PMO-8 (+6.1 vs +10.5 $^\circ\text{C}$). Unlike in the case of the guanidino G-clamp and the G-clamp, the substituent in the G^{SAE}-clamp may not reach guanines one step up and down from the opposite strand (C-[clamp]-C sequence context). This would explain the lack of additional stability—actually, there is a destabilization—afforded by a G^{SAE}-clamp wedged between cytosines. However, we hypothesize, as shown in Figure 2C, D, that the G^{SAE}-clamp, thanks to the orientation of its substituent, may enable favorable interactions with intrastrand 5'-G and 3'-G, respectively. This scenario remains to be tested.

Protonation of the G-clamp and the guanidino G-clamp can affect H-bonding with the complementary base as previously reported.²⁷ Lowering the pH decreased the T_m of duplexes between the unmodified PMO-1, PMO-6, and complementary DNA and RNA. The T_m values of duplexes formed with PMO-13 and PMO-14 modified with the G-clamp and the guanidinium G-clamp, respectively, were similar at neutral pH and at pH 5.5 and relatively higher at pH 4 than those of duplexes with unmodified PMO (Table 4, and Figures S29–S48). Presumably, protonation of the amines of the G-clamps at low pH results in stronger H-bonding interactions. However, in the case of PMO-4 and PMO-5, slight destabilization was observed with the RNA duplexes and a little bit of stabilization with DNA. On the contrary, both the phenoxazine and G8AE-clamp modified showed destabilization in PMO-2 and PMO-3, whereas relatively higher stabilization was observed in PMO-11 and PMO-12. This reflects the fact that the protonation of the flanked amine is not the sole parameter to control the duplex thermal stability but also the overall protonation of the strands and their composition.

Nucleobase recognition, which ensures the specificity of nucleic-acid-based drugs, is an important parameter during the characterization of novel modifications. We therefore determined the effects of mismatched bases on the target strands opposite the modified site. All mismatches significantly reduced the stabilities of duplexes of RNA and DNA with PMO-6, the unmodified oligomer, and with PMO-11, 12, 13, 14, (which has a single phenoxazine, G8AE-clamp, G-clamp, and Guanidino-G-clamp modification, respectively), in comparison with a fully complementary strand (Table 5 and Figures S49–S60).

The global conformations of the duplexes of PMOs with DNA and RNA were evaluated by CD spectra at 10 $^\circ\text{C}$. All

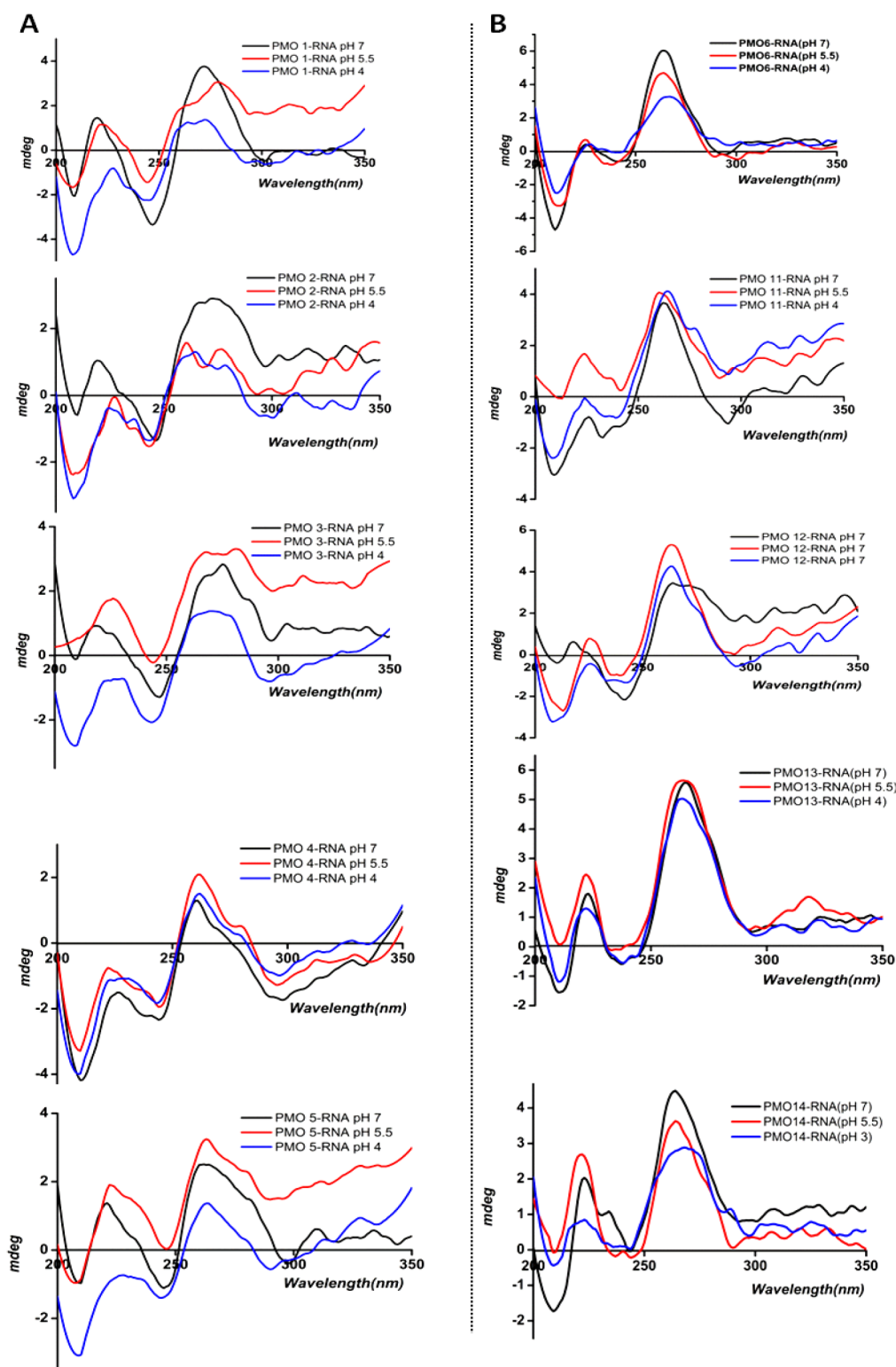


Figure 3. CD-spectra of (A) duplexes of PMO-1–5 with RNA, (B) duplexes of PMO-6 and PMO-11–14 with RNA at pH 7, 5.5, and 4.

duplexes with RNA had absorption maxima at approximately 270 and 220 nm with sharp minima at about 245 nm (Figure 3). Similar spectra were observed for duplexes with DNA (Figure S61). These spectra are typical of a B-type helical conformation for the PMO–DNA and PMO–RNA duplexes.

We also evaluated the CD spectra for the duplexes formed by the PMOs with RNA and DNA as a function of pH. In the CD spectra of the duplex of unmodified PMO-1 and PMO-6

with RNA, the intensity of the band at 265 nm was lower at pH 4 than at pH 7 (Figure 3). The probable cause is nucleobase protonation, although we cannot exclude the possibility of base pairing arrangements other than the standard Watson–Crick type.²⁷ In contrast, the spectra of the duplex of PMO-4 and PMO-13 (G-clamp incorporated PMOs) with RNA were similar at pH 4 and 7 (Figure 3). The protonation of the amine of the G-clamp moiety in an

oligomer at a lower pH will give rise to a more effective H-bonding interaction. Duplexes of PMO with DNA followed the same trends as a function of pH (Figures S62 and S63).

CONCLUSIONS

In summary, a convenient synthetic methodology was developed for the phenoxazine and its derivatives, the G^{SAE}-clamp, the G-clamp and guanidinium-G-clamp. The newly synthesized phenoxazine, G^{SAE}-clamp, G-clamp, and guanidino G-clamp PMO cytidines were incorporated into PMOs. Duplexes of PMOs with single modifications had higher thermal stabilities with the complementary DNA and RNA than the unmodified PMO. The duplexes of these modified PMOs with the complementary DNA and RNA possess a B-type helical structure as evidenced by CD spectroscopy. The aminoethoxy G-clamp tethered to the C8 and C9 of the tricyclic nucleobases show different melting behavior as expected due to the relative H-bonding abilities. The thermal stabilities of the duplexes were sequence-dependent. The guanidino G-clamp also stabilizes the duplex but the extent of stabilization varies depending upon the nature and position. Given the enhanced affinities of the G-clamp-modified PMO for RNA, this modification could allow the development of shorter PMOs than those currently in clinical use for splice modulation or might improve the potency of PMOs with the same length.

EXPERIMENTAL SECTION

Synthesis of Compound 1l. Portion (0.14 mmol) (120 mg) of compound 1k was dissolved in 3 mL of fresh dry DCM followed by the addition of LiBr (48 mg, 0.56 mmol). After that, 3 mL of fresh dry CH₃CN was added to the reaction mixture and cooled to 0 °C. 1,1,3,3-Tetramethylguanidine (71 μL, 0.56 mmol) was added dropwise. At last, POCl₂(NMe₂) was added dropwise to the reaction mixture and allowed to stir for 15 min. After consumption of the starting material (TLC analysis), the reaction mixture was diluted with cold DCM and transferred to the separating funnel. The organic layer was washed with a half-saturated NH₄Cl solution. The aqueous layer was extracted twice with DCM. The collected organic layer was dried over anhydrous Na₂SO₄ and dried in vacuo. The crude reaction mixture was purified immediately to obtain compound 1l as a bright yellow solid (R_f = 0.5 in 5% MeOH-DCM). Isolated yield = 67 mg, 0.065 mmol, 47%. ¹H NMR (300 MHz, Chloroform-*d*) δ 8.04 (s, 1H), 7.55–7.14 (m, 17H), 6.78 (d, J = 5.1 Hz, 1H), 6.52 (dd, J = 8.8, 1.8 Hz, 1H), 6.25 (dd, J = 9.1, 2.7 Hz, 1H), 6.10 (dd, J = 9.5, 2.3 Hz, 1H), 4.48–4.33 (m, 1H), 4.11 (ddt, J = 16.1, 12.1, 5.4 Hz, 4H), 3.71 (t, J = 5.0 Hz, 2H), 3.40 (d, J = 11.2 Hz, 1H), 3.16 (d, J = 11.6 Hz, 1H), 2.64 (dd, J = 13.8, 1.5 Hz, 6H), 1.46 (t, J = 10.7 Hz, 1H), 1.35–1.27 (m, 1H).

¹³C{¹H} NMR (75 MHz, CDCl₃) δ 158.0, 157.5, 154.9, 154.7, 153.5, 136.6, 129.2, 128.0, 126.7, 126.5, 121.6, 118.1, 115.8, 114.2, 110.6, 104.5, 81.2, 77.5, 77.3, 77.1, 77.0, 76.7, 74.5, 67.5, 66.4, 52.2, 49.1, 39.7, 36.7, 36.7. ³¹P NMR (121 MHz, CDCl₃) δ 18.29, 18.20. HRMS (ESI) [M + Na]⁺: Calcd mass for C₄₀H₃₉ClF₃N₆NaO₇P = 861.2156 found 861.2159.

Synthesis of Compound 2d. Compound 2d was synthesized from 2c (293 mg, 0.525 mmol) following the similar procedure described in 1l and isolated as a yellow solid. (R_f = 0.6 in 5% MeOH-DCM), isolated yield = 186 mg, 0.273 mmol, 52%. ¹H NMR (300 MHz, Chloroform-*d*) δ 7.73 (dd, J = 7.7, 1.7 Hz, 1H), 7.49 (d, J = 7.6 Hz, 5H), 7.41–7.14 (m, 10H), 6.99–6.78 (m, 3H), 6.65 (dd, J = 7.8, 1.5 Hz, 1H), 6.19 (dd, J = 9.3, 2.3 Hz, 1H), 4.42 (d, J = 9.9 Hz, 1H), 4.19–4.02 (m, 2H), 3.54–3.45 (m, 1H), 3.20–3.09 (m, 1H), 2.65 (d, J = 13.9 Hz, 6H), 1.46 (t, J = 11.1 Hz, 1H), 1.38–1.28 (m, 1H). ¹³C{¹H} NMR (75 MHz, CDCl₃) δ: 155.3, 153.3, 142.4, 129.3, 128.0, 127.8, 126.6, 126.3, 124.4, 124.0, 121.4, 118.5, 115.0, 81.5,

77.6, 77.4, 77.2, 77.0, 76.8, 74.7, 74.6, 67.5, 67.4, 52.2, 49.1, 38.7, 36.8, 36.7. ³¹P NMR (121 MHz, CDCl₃) δ 18.47, 18.19. HRMS(ESI) [M + Na]⁺: Calcd mass for C₃₆H₃₅ClN₅NaO₅P = 706.1962 found 706.1961.

Synthesis of Compound 3f. Compound 3f was synthesized from 3e (594 mg, 0.833 mmol) following the similar procedure described in 1l and isolated as a bright yellow solid. (R_f = 0.6 in 5% MeOH-DCM), isolated yield = 397 mg, 0.494 mmol, 57%. ¹H NMR (300 MHz, Chloroform-*d*) δ 8.90 (s, 1H), 7.53–7.12 (m, 16H), 6.81 (d, J = 9.5 Hz, 1H), 6.71 (t, J = 8.3 Hz, 1H), 6.38–6.28 (m, 2H), 6.12 (dd, J = 9.4, 2.3 Hz, 1H), 4.48–4.34 (m, 1H), 4.19–3.95 (m, 4H), 3.76 (d, J = 5.9 Hz, 2H), 3.41 (d, J = 11.3 Hz, 1H), 3.13 (d, J = 11.6 Hz, 1H), 2.64 (dd, J = 13.9, 4.8 Hz, 6H), 1.43 (t, J = 11.1 Hz, 1H), 1.29 (q, J = 2.9, 2.5 Hz, 1H). ¹³C{¹H} NMR (75 MHz, CDCl₃) δ: 158.2, 157.7, 153.2, 152.1, 146.5, 142.9, 129.2, 128.0, 127.4, 126.6, 124.5, 122.2, 118.0, 115.0, 114.2, 108.5, 106.7, 81.3, 77.5, 77.3, 77.1, 77.0, 76.7, 74.7, 74.6, 67.4, 67.1, 52.1, 49.0, 39.2, 36.7, 36.7. ³¹P NMR (121 MHz, CDCl₃) δ 18.48, 18.24. HRMS(ESI) [M + Na]⁺: Calcd mass for C₄₀H₃₉ClF₃N₆NaO₇P = 861.2156, found 861.2157.

ASSOCIATED CONTENT

Data Availability Statement

The data underlying this study are available in the published article and its Supporting Information.

Supporting Information

The Supporting Information is available free of charge at <https://pubs.acs.org/doi/10.1021/acs.joc.3c01658>.

Detailed experimental procedures and characterization data including the spectra for all new compounds (PDF)

AUTHOR INFORMATION

Corresponding Author

Surajit Sinha – School of Applied and Interdisciplinary Sciences, Indian Association for the Cultivation of Science, Kolkata 700032, India; orcid.org/0000-0001-8884-1194; Email: ocssS@iacs.res.in

Authors

Arnab Das – School of Applied and Interdisciplinary Sciences, Indian Association for the Cultivation of Science, Kolkata 700032, India

Atanu Ghosh – School of Applied and Interdisciplinary Sciences, Indian Association for the Cultivation of Science, Kolkata 700032, India

Jayanta Kundu – Alynlam Pharmaceuticals, Cambridge, Massachusetts 02142, United States

Martin Egli – Department of Biochemistry, School of Medicine, Vanderbilt University, Nashville, Tennessee 37232, United States; orcid.org/0000-0003-4145-356X

Muthiah Manoharan – Alynlam Pharmaceuticals, Cambridge, Massachusetts 02142, United States; orcid.org/0000-0002-7931-1172

Complete contact information is available at: <https://pubs.acs.org/doi/10.1021/acs.joc.3c01658>

Notes

The authors declare no competing financial interest.

ACKNOWLEDGMENTS

Part of the work of this manuscript has been deposited on the preprint server ChemRxiv.²⁸ S.S. thanks SERB, New Delhi, Government of India (Grant No. TTR/2021/000044) for financial support and the TRC facility at IACS for use of a

DNA synthesizer. A.D. and A.G. thank CSIR for their fellowships.

REFERENCES

- (1) Rinaldi, C.; Wood, M. J. A. Antisense oligonucleotides: the next frontier for treatment of neurological disorders. *Nat. Rev. Neurol.* **2018**, *14*, 9–21.
- (2) Sharma, V. K.; Sharma, R. K.; Singh, S. K. Antisense oligonucleotides: modifications and clinical trials. *Med. Chem. Commun.* **2014**, *5*, 1454–1471.
- (3) Crooke, S. T. Molecular mechanisms of action of antisense drugs. *Biochim. Biophys. Acta.* **1999**, *1489*, 31–44.
- (4) Crooke, S. T. Progress in antisense technology: the end of the beginning. *Methods Enzymol.* **2000**, *313*, 3–45.
- (5) Egli, M.; Manoharan, M. Re-engineering RNA molecules into therapeutic agents. *Acc. Chem. Res.* **2019**, *52*, 1036–1047.
- (6) Luyten, I.; Herdewijn, P. Hybridization properties of base-modified oligonucleotides within the double and triple helix motif. *Eur. J. Med. Chem.* **1998**, *33*, 515–576.
- (7) Saenger, W. *Principles of Nucleic Acid Structure*; Springer-Verlag: New York, 1984.
- (8) Yakovchuk, P.; Protozanova, E.; Frank-Kamenetskii, M. D. Base-stacking and base-pairing contributions into thermal stability of the DNA double helix. *Nucleic Acids Res.* **2006**, *34*, 564–574.
- (9) Petersheim, M.; Turner, D. H. Base-stacking and base-pairing contributions to helix stability: thermodynamics of double-helix formation with CCGG, CCGGp, CCGGAp, ACCGGp, CCGGUp, and ACCGGUp. *Biochemistry* **1983**, *22*, 256–263.
- (10) Hornum, M.; Djukina, A.; Sassnau, A.-K.; Nielsen, P. Synthesis of new C-5-triazolyl-functionalized thymidine analogs and their ability to engage in aromatic stacking in DNA: DNA and DNA: RNA duplexes. *Org. Biomol. Chem.* **2016**, *14*, 4436–4447.
- (11) Lin, K.-Y.; Jones, R. J.; Matteucci, M. D. Tricyclic 2'-deoxycytidine analogs: syntheses and incorporation into oligodeoxynucleotides which have enhanced binding to complementary RNA. *J. Am. Chem. Soc.* **1995**, *117*, 3873–3874.
- (12) Lin, K.-Y.; Matteucci, M. D. A cytosine analogue capable of clamp-like binding to a guanine in helical nucleic acids. *J. Am. Chem. Soc.* **1998**, *120*, 8531–8532.
- (13) Varizhuk, A. M.; Zatsepin, T. S.; Golovin, A. V.; Belyaev, E. S.; Kostyukevich, Y. I.; Dedkov, V. G.; Shipulin, G. A.; Shpakovski, G. V.; Aralov, A. V. Synthesis of oligonucleotides containing novel G-clamp analogue with C8-tethered group in phenoxazine ring: Implication to qPCR detection of the low-copy Kemerovo virus dsRNA. *Bioorg. Med. Chem.* **2017**, *25*, 3597–3605.
- (14) Ausin, C.; Ortega, J. A.; Robles, J.; Grandas, A.; Pedroso, E. Synthesis of amino-and guanidino-G-clamp PNA monomers. *Org. Lett.* **2002**, *4*, 4073–4075.
- (15) Ortega, J. A.; Blas, J. R.; Orozco, M.; Grandas, A.; Pedroso, E.; Robles, J. Binding affinities of oligonucleotides and PNAs containing phenoxazine and G-clamp cytosine analogues are unusually sequence-dependent. *Org. Lett.* **2007**, *9*, 4503–4506.
- (16) El-Sagheer, A. H.; Brown, T. Combined nucleobase and backbone modifications enhance DNA duplex stability and preserve biocompatibility. *Chem. Sci.* **2014**, *5*, 253–259.
- (17) Wild, C. J.; Maier, M. A.; Manoharan, M.; Egli, M. Structural Basis for Recognition of Guanosine by a Synthetic Tricyclic Cytosine Analogue: Guanidinium G-Clamp. *Helv. Chim. Acta* **2003**, *86*, 966–978.
- (18) Wild, C. J.; Maier, M. A.; Tereshko, V.; Manoharan, M.; Egli, M. Direct Observation of a Cytosine Analogue that Forms Five Hydrogen Bonds to Guanosine: Guanidino G-Clamp. *Angew. Chem., Int. Ed.* **2002**, *41*, 115–117.
- (19) Rajeev, K. G.; Maier, M. A.; Lesnik, E. A.; Manoharan, M. High-affinity peptide nucleic acid oligomers containing tricyclic cytosine analogues. *Org. Lett.* **2002**, *4*, 4395–4398.
- (20) Holmes, S. C.; Arzumanov, A. A.; Gait, M. J. Steric inhibition of human immunodeficiency virus type-1 Tat-dependent trans-activation in vitro and in cells by oligonucleotides containing 2'-O-methyl G-clamp ribonucleoside analogues. *Nucleic Acids Res.* **2003**, *31*, 2759–2768.
- (21) Kishimoto, Y.; Nakagawa, O.; Fujii, A.; Yoshioka, K.; Nagata, T.; Yokota, T.; Hari, Y.; Obika, S. 2', 4'-BNA/LNA with 9-(2-Aminoethoxy)-1, 3-diaza-2-oxophenoxazine Efficiently Forms Duplexes and Has Enhanced Enzymatic Resistance. *Chem.—Eur. J.* **2021**, *27*, 2427–2438.
- (22) (a) Summerton, J.; Weller, D. Morpholino antisense oligomers: design, preparation, and properties. *Antisense Nucleic Acid Drug Dev.* **1997**, *7*, 187–195. (b) Duan, D.; Goemans, N.; Takeda, S.; Mercuri, E.; Aartsma-Rus, A. Duchenne muscular dystrophy. *Nat. Rev. Dis. Primers* **2021**, *7*, 13. (c) Li, D.; Adams, A. M.; Johnsen, R. D.; Fletcher, S.; Wilton, S. D. Morpholino oligomer-induced dystrophin isoforms to map the functional domains in the dystrophin protein. *Mol. Ther. Nucleic Acids* **2020**, *22*, 263–272. (d) Corey, D. R.; Abrams, J. M. Morpholino antisense oligonucleotides: tools for investigating vertebrate development. *Genome Biol.* **2001**, *2*, 1015.1–1015.3, DOI: 10.1186/gb-2001-2-5-reviews1015. (e) Summerton, J. Morpholino antisense oligomers: the case for an RNase H-independent structural type. *Biochim. Biophys. Acta* **1999**, *1489* (1), 141–158. (f) Du, L.; Gatti, R. A. Potential therapeutic applications of antisense morpholino oligonucleotides in modulation of splicing in primary immunodeficiency diseases. *J. Immunol. Methods* **2011**, *365* (1), 1–7.
- (23) Paul, S.; Pattanayak, S.; Sinha, S. Synthesis and cell transfection properties of cationic uracil-morpholino tetramer. *Tetrahedron Lett.* **2014**, *55*, 1072–1076.
- (24) Das, A.; Ghosh, A.; Sinha, S. C5-pyrimidine-functionalized morpholino oligonucleotides exhibit differential binding affinity, target specificity and lipophilicity. *Org. Biomol. Chem.* **2023**, *21*, 1242–1253.
- (25) Kundu, J.; Ghosh, A.; Ghosh, U.; Das, A.; Nagar, D.; Pattanayak, S.; Ghose, A.; Sinha, S. Synthesis of phosphorodiamidate morpholino oligonucleotides using trityl and fmoc chemistry in an automated oligo synthesizer. *J. Org. Chem.* **2022**, *87*, 9466–9478.
- (26) Maier, M. A.; Barber-Peoc'h, I.; Manoharan, M. Postsynthetic guanidinylation of primary amino groups in the minor and major grooves of oligonucleotides. *Tetrahedron Lett.* **2002**, *43*, 7613–7616.
- (27) Mariani, A.; Bonfio, C.; Johnson, C. M.; Sutherland, J. D. pH-Driven RNA strand separation under prebiotically plausible conditions. *Biochemistry* **2018**, *57* (45), 6382–6386.
- (28) Sinha, S.; Das, A.; Ghosh, A.; Kundu, J.; Egli, M.; Manoharan, M. Synthesis and Biophysical Studies of High Affinity Morpholino Oligomers Containing G-clamp Analogs. *ChemRxiv* **2023**, DOI: 10.26434/chemrxiv-2023-fhfr.